American Mineralogist, Volume 79, pages 15–23, 1994

High-pressure X-ray diffraction study of carbonates: $MgCO_3$, $CaMg(CO_3)_2$, and $CaCO_3$

Guillaume Fiquet
Ecole Normale Supérieure de Lyon, Laboratoire de Sciences de la Terre, URA CNRS 726,
46 Allée d'Italie, 69364 Lyon Cedex 07, France

François Guyot
Institut de Physique du Globe de Paris, Laboratoire de Physique des Géomatériaux, URA CNRS 734,
4 Place Jussieu, 75252 Paris Cedex 05, France

Jean-Paul Itié
Laboratoire des Milieux Condensés, URA CNRS 782, Université Pierre et Marie Curie,
4 Place Jussieu, 75252 Paris Cedex 05, France

Abstract

High-pressure X-ray powder diffraction data on $MgCO_3$, $CaMg(CO_3)_2$, and $CaCO_3$ have been collected up to 53, 11, and 18 GPa, respectively. Patterns were recorded in a diamond-anvil cell in an energy-dispersive configuration at the storage ring DCI at the LURE (Orsay, France). Anisotropic compression of the unit-cell parameters is observed for dolomite and magnesite, with the *c* axis three times more compressible than the *a* axis. The greater compressibility of the *c* axis can also be observed in calcite I. Assuming $K_0' = 4$, we obtain bulk moduli from fits of the pressure-volume data to a second-order Eulerian finite strain equation of state equal to $K_0 = 112.9 \pm 2.2$ GPa for dolomite and $K_0 = 137.5 \pm 3.2$ GPa for magnesite. At 25 GPa, the appearance of new diffraction peaks and the presence of anomalies in the compression curve suggest the occurrence of a phase change in magnesite.

The high-pressure polymorphs of calcite coexist in reduced pressure ranges, suggesting an important hysteresis for phase changes of calcite at high pressure and ambient temperature. In single-phase domains, it is possible to determine the isothermal bulk moduli of calcite I and calcite III. Assuming $K_0' = 4$, one obtains $K_0 = 69.5 \pm 2.1$ GPa for calcite I and $K_0 = 93.2 \pm 1.9$ GPa, associated with an ambient pressure volume $V_0 = 31.87 \pm 0.17$ cm³/mol, for calcite III. The relative volume change at the transition between calcite I and calcite II is very small ($\Delta V/V = -1\%$), whereas it is much larger between calcite II and calcite III ($\Delta V/V = -15\%$).

Introduction

The behavior of carbonates at high pressures and temperatures has profound implications for the global C cycle and the buffering of f_{O_2} at depth. High-pressure polymorphs of carbonates could indeed be the host phases of oxidized C in the Earth's mantle. Carbonates have been shown, for example, to be stable at high pressures and temperatures by Irving and Wyllie (1975) and more recently by Kraft et al. (1991), Canil and Scarfe (1990), or Katsura and Ito (1990). The recent observations of Biellmann et al. (1992, 1993) confirmed that magnesite is stable at 40 GPa and 2000 K in the presence of silicates, opening new perspectives on the storage of C in the Earth's lower mantle. However, relatively little is known about the structural properties of carbonates at high pressures and temperatures. Room-pressure high-temperature crystal structures have been refined for calcite, magnesite, and dolomite (Markgraf and Reeder, 1985; Reeder and Markgraf, 1986). On the other hand, high-pressure studies of carbonates have been mostly devoted to calcite (Bridgman, 1939; Davis, 1964; Vaidya et al., 1973; Singh and Kennedy, 1974; Merrill and Bassett, 1975), except in the high-pressure X-ray study of Martens et al. (1982) performed on witherite ($BaCO_3$), strontianite ($SrCO_3$), rhodochrosite ($MnCO_3$), and calcite III ($CaCO_3$). For magnesium and iron carbonates, elastic properties are available from Christensen (1972) and Kalashnikov et al. (1973). Recently, high-pressure Raman studies have been performed on magnesite and calcite polymorphs by Williams et al. (1992) and on calcite, magnesite, dolomite, and aragonite by Gillet et al. (1993). Room-temperature high-pressure crystal structure refinements have also been done by Ross and Reeder (1992) on dolomite and ankerite, and the compression of magnesite has been recently studied by Redfern et al. (1993). In order to bring new insights on stability and properties of carbonates at high pressure, we report the compression of magnesite and dolomite up to 53 and 11 GPa, respectively. In addition, the compression of calcite I, II, and III up to 18 GPa is presented.

0003–004X/94/0102–0015$02.00

TABLE 1. Unit-cell parameters of dolomite as a function of pressure

P (GPa)	a (Å)	c (Å)	V (Å³)
0.0	4.830(3)	16.01(1)	323.2(4)
0.2	4.822(3)	16.01(1)	322.2(4)
1.1[1]	4.817(4)	15.93(1)	319.9(6)
1.8[1]	4.814(1)	15.88(1)	318.5(2)
2.7[2]	4.803(8)	15.85(2)	316.5(10)
3.6[2]	4.791(3)	15.76(1)	313.0(4)
5.5[3]	4.780(5)	15.66(1)	309.8(6)
6.5[4]	4.773(9)	15.58(3)	307.3(11)
7.1[4]	4.769(9)	15.54(3)	305.9(11)
8.5[5]	4.764(5)	15.43(1)	303.2(6)
9.2[6]	4.758(5)	15.43(1)	302.4(6)
9.8[6]	4.755(10)	15.41(3)	301.5(12)
10.9[7]	4.753(8)	15.29(2)	299.0(8)

Note: pressure uncertainty in brackets, standard deviations in parentheses.

TABLE 2. Unit-cell parameters of magnesite as a function of pressure

P (GPa)	a (Å)	c (Å)	V (Å³)
0.00	4.635(2)	15.03(1)	279.7(3)
1.4[1]	4.621(2)	14.95(1)	276.5(3)
2.0[2]	4.616(2)	14.91(1)	275.0(2)
2.6[2]	4.613(3)	14.89(1)	274.3(4)
3.6[2]	4.606(3)	14.84(2)	272.6(4)
4.8[3]	4.594(3)	14.79(2)	270.4(5)
5.6[4]	4.593(4)	14.76(2)	269.7(6)
6.1[5]	4.592(4)	14.74(2)	269.2(6)
7.4[5]	4.584(5)	14.70(3)	267.4(8)
8.1[5]	4.575(7)	14.67(3)	266.0(10)
8.5[5]*	4.588(2)	14.47(2)	263.8(5)
9.5[6]	4.567(8)	14.63(4)	264.3(12)
10.1[6]	4.567(8)	14.59(4)	263.5(12)
10.9[7]	4.563(7)	14.54(4)	262.2(10)
11.7[7]	4.566(9)	14.46(5)	261.1(14)
12.3[7]	4.559(9)	14.45(4)	260.1(13)
13.8[8]	4.558(7)	14.36(3)	258.4(10)
15.3[9]	4.549(9)	14.34(5)	257.0(14)
16.0[12]*	4.555(12)	14.31(11)	257.1(26)
24.0[18]*	4.510(10)	14.08(4)	247.9(13)
24.7[13]*	4.497(11)	14.05(6)	245.9(17)
25.3[11]*	4.467(9)	13.93(5)	240.6(13)
29.5[18]*	4.458(6)	13.26(6)	228.2(13)
48.0[20]*	4.383(8)	13.15(8)	218.6(17)
52.7[35]*	4.387(5)	13.05(5)	217.4(11)

Note: pressure uncertainty in brackets, standard deviations in parentheses.
*Denotes a second series of experiments performed at higher pressures.

EXPERIMENTAL METHODS

Samples

Dolomite and magnesite samples were carefully selected from clear crystals, free from inclusions, kindly provided by the University of Rennes (France). The dolomite sample used in this study was taken from a cleavage of Eugui dolomite, which shows a nearly ideal composition, $Ca_{1.001}Mg_{0.987}Fe_{0.010}Mn_{0.002}(CO_3)_2$, as reported in the earlier high-temperature study of Reeder and Wenk (1983). The magnesite specimen was taken from a clear cleavage rhomb of Bahia magnesite, a sample also selected for its high-quality crystals and because it was used in the study of elastic properties of Humbert and Plicque (1972). The calcite sample was pure reagent-grade $CaCO_3$ from Merck. The ambient pressure and temperature X-ray powder diffraction patterns of the three compounds, very close to the JCPDS cards, showed samples to be single-phase materials and do not warrant particular comments.

High-pressure diffraction experiments

The samples were ground into micrometer-sized crystals and loaded in a diamond-anvil cell equipped with 600-μm culets. The gasket was made with 301 stainless steel drilled with a hole 200 μm in diameter. The sample and several tiny crystals of ruby were mounted in a silicone oil (dimethylpolysiloxane—ref. 47V1000—from Prolabo), used as a pressure transmitting medium. Pressures were measured with the ruby fluorescence method. A second series of experiments was also carried out at higher pressure for magnesite, in a diamond-anvil cell equipped with 400-μm culets. Silicone oil was used as a pressure transmitting medium in this series, except for the experiments at 8.5, 16.0, and 24.7 GPa, in which LiF (spectroscopic grade, Prolabo) was employed. For all experiments, fluorescence line profiles are used to monitor quasi-hydrostatic conditions up to 15 GPa. In this study, the errors on the pressure measurements due to reading uncertainties do not exceed 10% of the pressure value (see Tables 1, 2, and 3), and they include errors due to pressure variations across the X-rayed spot, assumed to broaden the ruby fluorescence peaks. High-pressure powder X-ray measurements were then conducted at ambient temperature in an energy-dispersive mode at the storage ring DCI (LURE, Orsay, France). The samples were X-rayed in the diamond-anvil cell by a polychromatic X-ray beam, collimated by a remote tungsten carbide slit system to a spot 50 × 50 μm strictly centered on the pressure chamber. The diffracted beam was analyzed at 11.329° 2θ between 5 and 50 keV by a Canberra planar Ge detector (efficient area 50 mm²), with a resolution between 145 eV at 5.9 keV and 500 eV at 122 keV. We used a large sample-detector distance combined with a 100-μm detector entrance slit and a 2θ defining slit system, thus allowing us to record the patterns with a resolution close to the theoretical capabilities of the detector.

Lattice parameter refinements and equations of state

The lattice parameters were calculated with a least-squares program adapted from an initial version called LCR2. Hexagonal symmetry was used for the refinement of the unit-cell parameters of dolomite, magnesite, and calcite. Monoclinic and orthorhombic configurations were then respectively used for calcite II and III, in accordance with Merrill and Bassett (1975) and Davis (1964). Standard deviations were calculated for each parameter, assuming a constant ±60 eV (i.e., 10^{-2} Å) reading uncertainty for each line. For dolomite and magnesite, five intense reflections could be read up to the maximum pressures achieved and were used in the refinements. Six reflections were taken into account for calcite I and calcite II, whereas five were used for calcite III.

TABLE 3. Unit-cell parameters of calcite as a function of pressure

P (GPa)	*a* (Å)	*b* (Å)	*c* (Å)	β (°)	*V* (Å³)
			Calcite I, hexagonal system, *Z* = 6		
0	4.990(1)		17.06(1)		368.0(5)
0.9[1]	4.974(2)		16.94(1)		362.9(5)
1.2[1]	4.968(3)		16.97(3)		362.6(9)
1.4[1]	4.966(4)		16.91(2)		361.0(8)
1.6[1]	4.961(4)		16.88(2)		359.8(8)
1.8[1]	4.959(5)		16.89(5)		359.6(14)
			Calcite II, monoclinic system, *Z* = 4		
1.6[1]	6.29(2)	4.99(1)	7.95(2)	106.8(2)	238.8(18)
1.6[1]	6.28(4)	4.99(2)	7.91(4)	106.7(4)	237.4(33)
1.8[1]	6.27(1)	4.99(1)	7.91(1)	106.7(1)	236.8(11)
			Calcite III, orthorhombic system, *Z* = 10		
2.3[1]	8.75(5)	8.37(4)	7.08(9)		518.3(116)
2.6[1]	8.75(9)	8.36(9)	7.06(4)		516.1(138)
3.5[2]	8.63(5)	8.34(2)	7.07(3)		508.4(68)
4.1[2]	8.60(5)	8.33(2)	7.05(3)		505.3(69)
5.0[3]	8.62(4)	8.30(2)	7.03(2)		502.9(48)
6.0[3]	8.60(5)	8.26(2)	7.05(3)		500.4(64)
6.8[3]	8.50(1)	8.27(1)	7.08(1)		497.5(11)

Note: pressure uncertainty in brackets, standard deviations in parentheses.

The measurements of the unit-cell parameters were then fitted to an Eulerian finite strain equation of state, that is

$$P = \tfrac{3}{2}K_0[(V_0/V)^{7/3} - (V_0/V)^{5/3}] \cdot\{1 + \tfrac{3}{4}(K_0' - 4)[(V_0/V)^{2/3} - 1]\}$$

to third order in energy, the so-called Birch-Murnaghan equation of state. The bulk modulus K_0, its first pressure derivative K_0', the reference volume V_0, and associated errors were then determined using a program developed by Ross and Webb (1989). The calculated errors on these parameters include both volume and pressure measurement uncertainties.

Results and discussion

Dolomite and magnesite

The unit-cell parameters of dolomite and magnesite are given as a function of pressure in Tables 1 and 2. Room-pressure patterns of both compounds were first recorded in the diamond-anvil cell to determine the reference volumes. The room-pressure parameters of dolomite, a = 4.8298(26), c = 16.005(12), show a reasonable agreement with those given by Ross and Reeder (1992), a = 4.8064(5) and c = 16.006(2) Å. The parameters of magnesite, a = 4.6348(20), c = 15.034(11), compare well with those given by Markgraf and Reeder (1985), a = 4.635(2) and c = 15.019(3) Å. After decompression, dolomite and magnesite were recovered with their initial structures and parameters, although some diffraction lines were broadened, especially 006 and 116.

The axial compressions a/a_0 and c/c_0 are plotted as a function of pressure in Figure 1. The c axis is about three times more compressible than the a axis, in agreement with the results obtained by Ross and Reeder (1992) for dolomite and ankerite. A larger compressibility for the c axis in magnesite was also measured by Katsura et al. (1991). Linear regressions yield mean axial compressibilities for a and c equal to 1.48×10^{-3} and 4.01×10^{-3}/GPa, and 1.08×10^{-3} and 2.66×10^{-3}/GPa for dolomite and magnesite, respectively. The compressibilities obtained for dolomite are slightly smaller than those measured by Ross and Reeder (1992), which might be because of the larger pressure range investigated in our experiments.

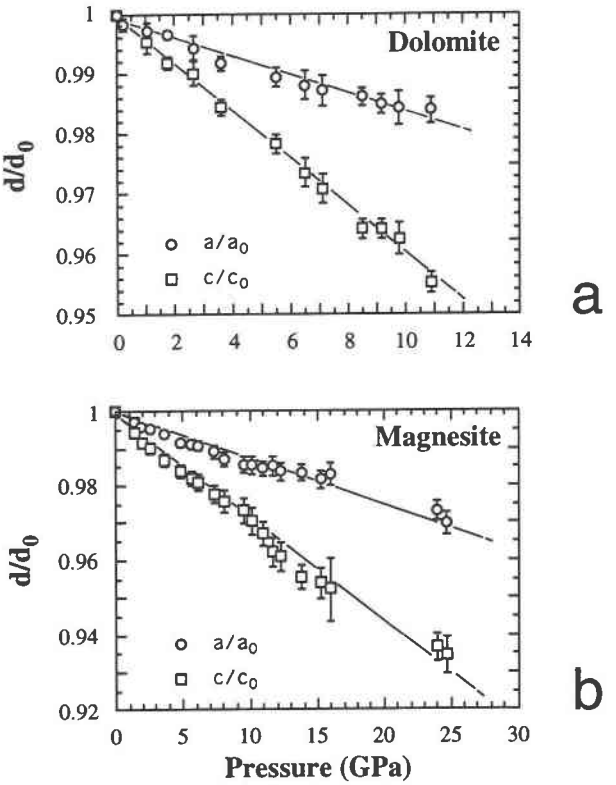

Fig. 1. Axial compressions a/a_0 and c/c_0 as a function of pressure in dolomite up to 11 GPa (**a**) and in magnesite up to 25 GPa (**b**). Lines represent linear fits. Pressures are measured with a maximum relative error of ±5%.

Calcite

The unit-cell parameters of the various polymorphs are listed as a function of pressure in Table 3. For calcite I, the ambient pressure values a = 4.9904(12) and c = 17.064(7), obtained from a zero-pressure spectrum recorded in the diamond-anvil cell, agree well with those given by Markgraf and Reeder (1985), a = 4.988(1) and c = 17.061(1) Å. After decompression, calcite was recovered with its initial structure and parameters, but with some line broadening affecting principally 006 and 116, as in magnesite and dolomite.

The axial compressions a/a_0 and c/c_0 of calcite I are plotted as a function of pressure in Figure 2. Despite large error bars and a small pressure range, the larger compressibility of the c axis is evident, as in magnesite and dolomite. Linear regressions yield mean axial compressibilities of 3.55×10^{-3} and 5.96×10^{-3}/GPa for a and

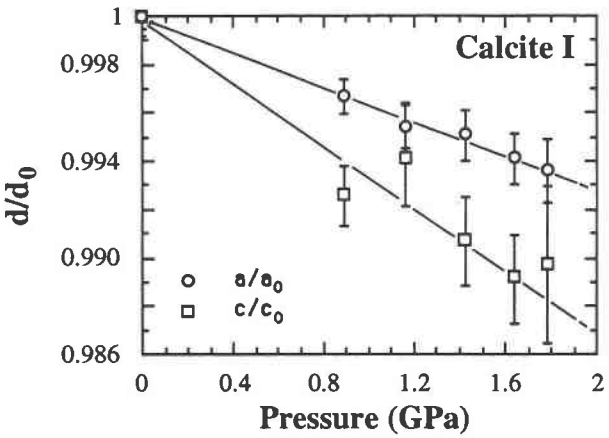

Fig. 2. Axial compressions a/a_0 and c/c_0 as a function of pressure for calcite I. Lines represent linear fits.

c, respectively. These mean values are larger than those obtained for dolomite and magnesite partly because of the smaller pressure range investigated. The lattice parameters of calcite III are represented as a function of pressure in Figure 3. The b axis is clearly more compressible than the a axis, whereas the c axis is rather incompressible. No significant change of the calcite II axes could be measured in the reduced pressure range over which this phase could be detected.

Compression anisotropy

Magnesite and calcite I structures are consistent with the $R\bar{3}c$ space group. In dolomite, the presence of more than one divalent cation, namely Ca^{2+} and Mg^{2+}, ordered in alternating layers with the CO_3^{2-} group, leads this carbonate to adopt the $R\bar{3}$ symmetry. All these structures can be described as distortions of a (B1) NaCl structure (e.g., Wells, 1984). A convenient parameter to describe the degree of distortion from the NaCl structure is $t = 4a/\sqrt{2}c$ where a and c are the lattice parameters. This parameter t would be equal to one in an ideal NaCl structure. In carbonates, values of $t = 0.849$ for dolomite, $t = 0.873$ for magnesite, and $t = 0.827$ for calcite are obtained at room pressure and temperature. Structurally, the a parameter is related to a M^{2+}-M^{2+} distance and c to a M^{2+}-CO_3^{2-} distance. Obviously, the low t values show that carbonates are less compact along the **c** axis than the **a** axis. This could partly explain the differences in relative compressibilities between these two axes. The values of the compressibilities are largely determined by the polarizability of the cations, which decreases from Ca to Mg, explaining why dolomite is more compressible than magnesite. Calcite I is probably more compressible than these two compounds, but the comparison is difficult because of the small pressure range over which it was investigated. A similar sequence of compressibilities was also described by Martens et al. (1982) for $BaCO_3$, $SrCO_3$, and $MnCO_3$.

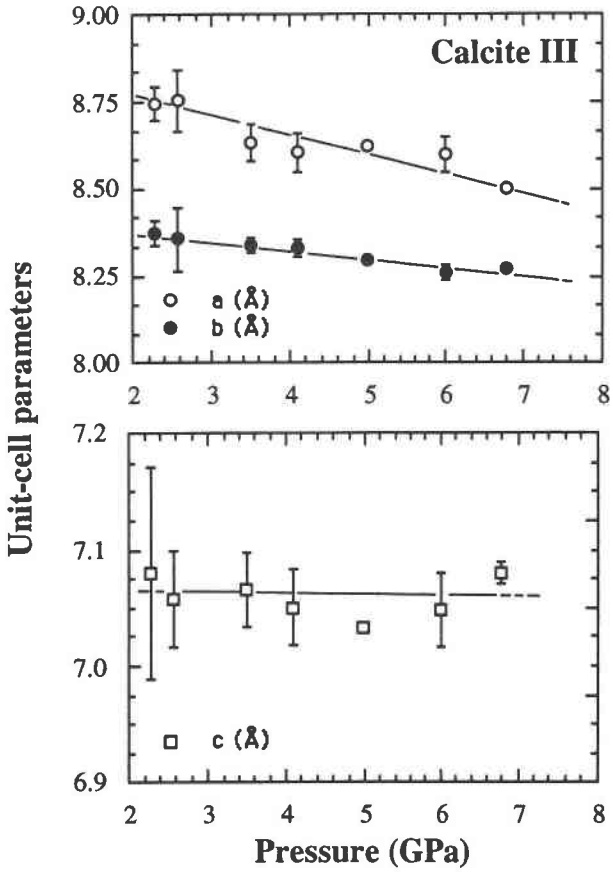

Fig. 3. Unit-cell parameters of calcite III as a function of pressure. Lines represent linear fits.

Bulk moduli of dolomite and magnesite

Molar volumes of dolomite and magnesite are represented in Figures 4 and 5 as a function of pressure. The smooth high-pressure behavior of dolomite does not warrant particular comments, and a single equation of state can be proposed up to 11 GPa. A single equation of state can also be proposed for magnesite up to 53 GPa, although new features, suggesting a phase change discussed below, appear in the X-ray patterns at pressures exceeding 25 GPa. We will thus also propose a separate equation of state for magnesite only up to 25 GPa.

The refined equation of state parameters are reported for dolomite and magnesite in Table 4. Setting V/V_0 equal to 1, one obtains $K_0 = 96.0 \pm 5.2$ GPa, $K_0' = 10.0 \pm 2.2$, and $K_0 = 155.7 \pm 3.9$ GPa, $K_0' = 2.5 \pm 0.2$ for dolomite and magnesite, respectively. The values given for K_0' are only approximate because of the extensive trade-off between K_0 and K_0', easily explained by the small pressure range investigated. In such cases, K_0' may rather be an adjustable parameter than the actual room-pressure derivative of K. Reasonable fits can also be obtained with a fixed value of 4 for K_0', leading K_0 to be equal to 112.9 $\pm$ 2.2 and 137.5 $\pm$ 3.2 GPa for dolomite and magnesite, respectively. Results obtained for dolomite compare rea-

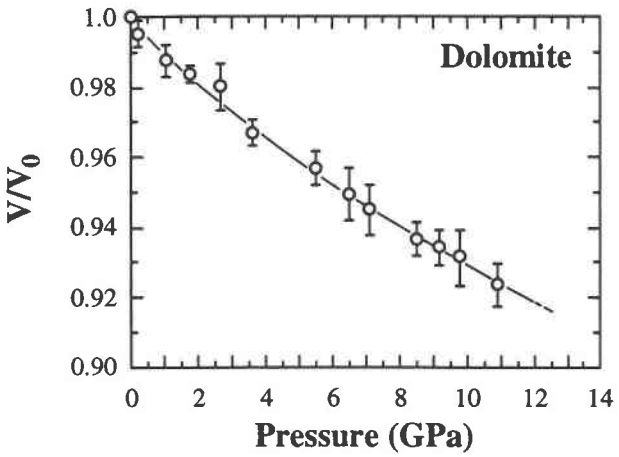

Fig. 4. Room-temperature compression of dolomite as a function of pressure. The line represents the equation of state best fit.

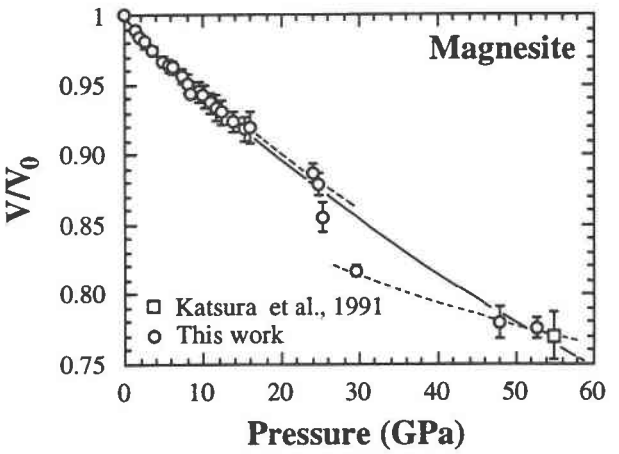

Fig. 5. Room-temperature compression of magnesite as a function of pressure. The solid line represents the equation of state best fit, the dashed line a separate fit, with a possible phase transition at 25 GPa.

sonably well with values of K_0 = 94.1(7) with K_0' = 4, obtained by Ross and Reeder (1992), and K_{S_0} = 94.9 GPa derived from the single-crystal acoustic measurements of Humbert and Plicque (1972). Our values of K_0 for magnesite are significantly larger than the values of the adiabatic bulk moduli of K_{S_0} = 112 and 113.8 GPa reported in the studies of Christensen (1972) and Humbert and Plicque (1972). On the other hand, our results show a reasonable agreement with the static compression study of Redfern et al. (1993), who propose 142 GPa for K_0, with a fixed value of 4 for K_0'. Applying a full Birch-Murnaghan equation of state, they obtain K_0 = 151 GPa and K_0' = 2.5, values close to our K_0 = 155.7 GPa and K_0' = 2.5.

Existence of a high-pressure phase of magnesite

As mentioned previously, changes in the X-ray patterns and anomalies in the compression curve are observed at pressures exceeding 25 GPa. As shown in Figure 6, the four major diffraction lines of magnesite, namely 104, 110, 113, and 022, can be recognized. Above 25 GPa, however, the X-ray patterns differ slightly (Fig. 6). A shoulder occurs on the high-energy side of 104 (corresponding to a smaller *d*-value reflection), and a new peak appears between 104 and 110; there might also be some additional peaks at lower energy (or greater *d* values). Moreover, the refinement of the unit-cell parameters in the magnesite structure suggests that changes occur above 25 GPa (Fig. 7). Therefore, we propose a separate equation of state for magnesite up to 25 GPa only, with K_0 = 131.9 ± 3.1 GPa and K_0' = 7.5 ± 0.7. Assuming K_0' = 4, one obtains K_0 = 147.2 ± 2.1 GPa.

No phase transition in magnesite has been reported in previous studies. The shock measurements of Kalashnikov et al. (1973) to 120 GPa did not mention any change in the slope between the shock wave velocity and the particle velocity of magnesite. No phase transition was reported in the Raman studies of Williams et al. (1992) to 34 GPa and Gillet (1993) to 32 GPa and high-temperature. Katsura et al. (1991) reported an unchanged magnesite structure in their X-ray diffraction measurement at 55 GPa. The meaning of the changes observed above 25 GPa in this study thus remains unclear, and

TABLE 4. Equation of state parameters of dolomite and magnesite

Reference	K_0 (GPa)	K_0'	*Method*
	Dolomite		
Humbert and Plicque (1972)*	94.9–90.2	—	acoustic
Ross and Reeder (1992)	94.1 ± 0.7	4	X-ray
Eulerian, second-order	112.9 ± 2.2	4	this work
Eulerian, third-order	96.0 ± 5.2	10.0 ± 2.2	this work
	Magnesite		
Christensen (1972)*	112	—	acoustic
Humbert and Plicque (1972)*	113.8–109.9	—	acoustic
Redfern et al. (in preparation)	142	4	X-ray
	151	2.5	idem
Eulerian, second-order	137.5 ± 3.2	4	this work**
Eulerian, third-order	155.7 ± 3.9	2.5 ± 0.2	this work**

* Adiabatic bulk moduli.
** The experimental points at 25.3 and 29.5 GPa are not included in this refinement.

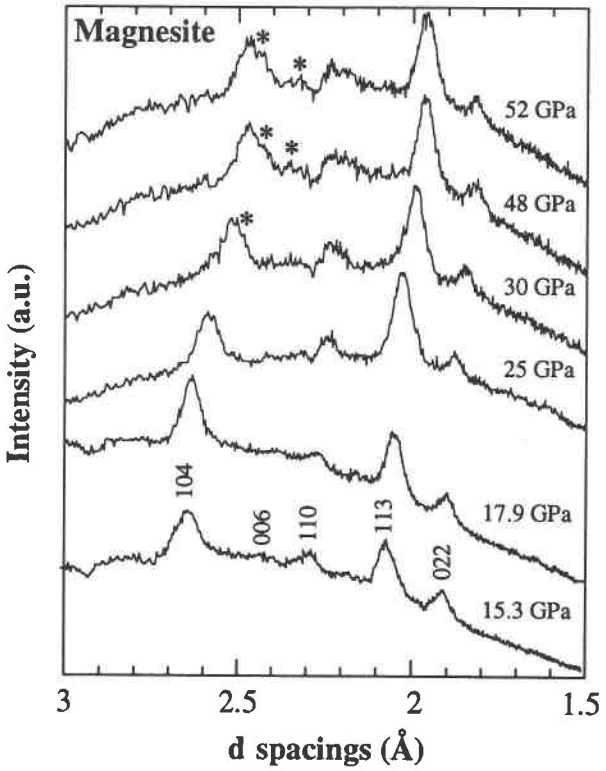

Fig. 6. Evolution of the X-ray powder diffraction patterns of magnesite at pressures exceeding 15 GPa. Asterisks denote new features above 25 GPa, mainly a shoulder growing in the 104 peak and a small but significant line appearing between the 104 and 006 reflections. Patterns have been represented as a function of *d* values (instead of energy) to keep a single scale up to 53 GPa.

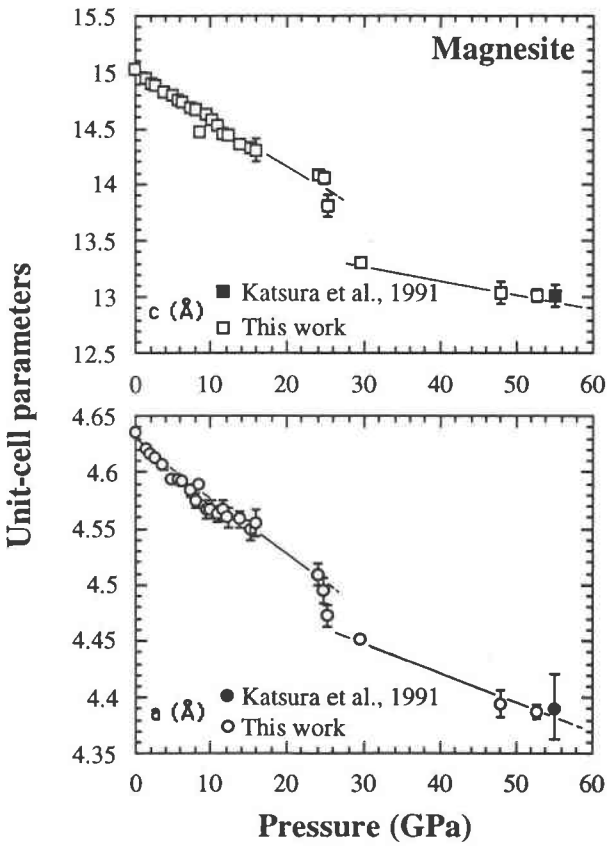

Fig. 7. Unit-cell parameters of magnesite as a function of pressure. Lines represent linear fits to the data before and after the anomalies at 25 GPa.

further high-pressure studies are needed to resolve this issue.

Changes in the compression mechanism

Additional minor changes can be detected in the low-pressure range for dolomite and magnesite. Breaks in the compression curves appear in magnesite at 8 GPa and in dolomite at 4 GPa. These breaks are particularly visible in the dependence of the cell parameters on pressure (Fig. 8). Obviously, the *c* axis of magnesite becomes more compressible at pressures exceeding 8 GPa, whereas the *a* axis seems to become less compressible above this pressure (Fig. 8a). Such a dependence is less obvious for dolomite, but the same behavior can be considered at 4 GPa (Fig. 8b). However, no significant changes are observed in the X-ray patterns, suggesting that these features could be better understood as a change in the compression mechanism. Alternatively, they could be due to a second-order transition like the one observed in $NaNO_3$ by Lettieri et al. (1978), which is associated with pressure-induced freezing of rotation modes of the NO_3^- groups. Our data show that such a change occurs at lower pressure in dolomite than in magnesite, in agreement with the empirical rule asserting that high-pressure transformations occur at lower pressure in oxides containing larger cations. The Raman studies of Kraft et al. (1991) on dolomite, Williams et al. (1992) on magnesite, and Gillet et al. (1993) did not mention any major modification of the Raman spectra of magnesite and dolomite with increasing pressure nor any change in the slopes of frequency shifts vs. pressure. No change is reported for dolomite in the high-pressure X-ray single-crystal refinement of Ross and Reeder (1992), but the maximum pressure of their study is that at which changes are observed in this work. This comparison with previous data shows that these effects are small.

The effect of such kinks on the equation of state parameters is minor. However, it is possible to derive K_0 in domains preceding and following the kinks. Assuming a K_0' value of 4, one obtains K_0 values of 102(5) and 116(1) GPa before and after the kink in dolomite, whereas K_0 = 139(4) and 149(1) GPa before and after the kink in magnesite.

Calcite polymorphism

At high pressures and room temperature, calcite I undergoes a series of phase transitions. According to Bridg-

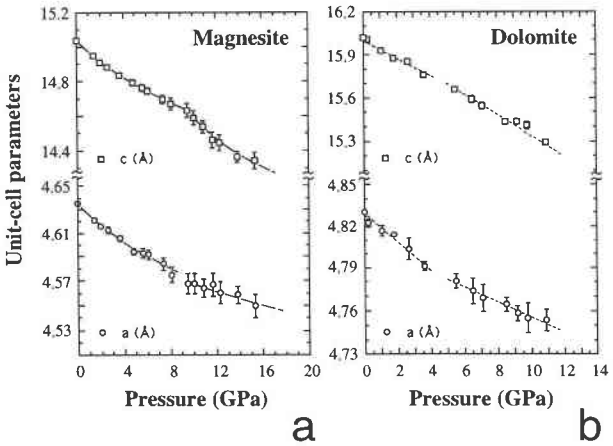

Fig. 8. (**a**) Unit-cell parameters of magnesite as a function of pressure up to 25 GPa. Lines represent best fits to the data. (**b**) Unit-cell parameters of dolomite as a function of pressure. Dashed lines represent linear fits to the data.

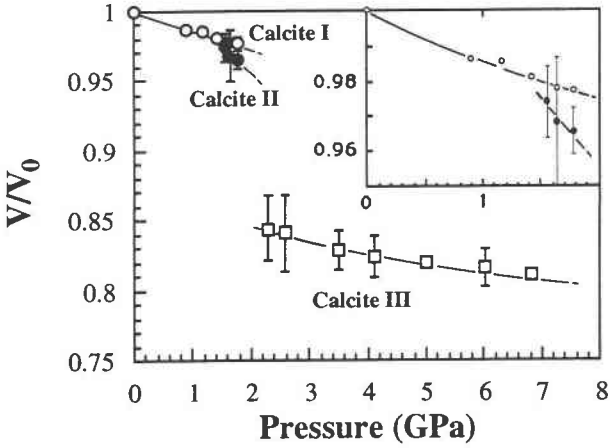

Fig. 9. Room-temperature compression of calcite I, II, and III as a function of pressure. Lines represent the equations of state for calcite I and calcite III, and a linear fit for calcite II. The domain of calcite I + calcite II coexistence is shown enlarged.

man (1939) and Singh and Kennedy (1974), these transitions are thought to occur at 1.45 and 1.74 GPa for calcite I → calcite II and calcite II → calcite III, respectively. Merrill and Bassett (1975) stated that these values were revised to 1.5 and 2.2 GPa, respectively. The exact structures of the high-pressure polymorphs are still debated. For calcite II, we have chosen the monoclinic structure proposed by Merrill and Bassett (1975) from a single-crystal X-ray study. Calcite II differs slightly from calcite I by a rotation of the CO_3^{2-} planar groups and a small displacement of the Ca^{2+} cations. The structure of calcite III is not so well known, and several authors have proposed a monoclinic structure (Merrill and Bassett, 1972; Williams et al., 1992). In this study, we follow the orthorhombic assignment of Davis (1964). The reasons for this choice are double: first, the observed lines can be indexed as this phase; second the reduced number of observed lines makes inappropriate the assignment into a lower symmetry structure. Davis (1964) proposed that calcite III is isomorphic with KNO_3 IV, which is itself related to NH_4NO_3 III, a distorted form of a (B2) CsCl structure.

In Figure 9, we have plotted the volume of the calcite polymorphs as a function of pressure. It is apparent that the ΔV between calcite I and calcite II is very small ($\Delta V/V = -1\%$). Such a result is consistent with the studies of Singh and Kennedy (1974) and Vo Thanh and Lacam (1984), which gave values of -1.3 and -1.7%, respectively. The structural similarity between calcite I and II explains such a small transition volume. On the other hand, the large volume change observed between calcite I and II and calcite III ($\Delta V = -4.2$ cm³/mol, $\Delta V/V = -15\%$) is consistent with volume changes of transitions of B1 → B2 type. For example, the rock salt phase of SrO transforms near 36 GPa to a CsCl-type structure with a $\Delta V/V = -13\%$ (Sato and Jeanloz, 1981). The transition from rock salt to CsCl reported for CaO in the range 60–70 GPa is also accompanied by a -11% change in volume (Jeanloz et al., 1979; Richet et al., 1988). In previous studies, a larger volume change was usually attributed to the calcite I → calcite II transition and a smaller one to the calcite II → calcite III transition (Bridgman, 1939; Singh and Kennedy, 1974). The discrepancy may be at least partly explained by the existence of strong hysteresis phenomena. We have indeed observed the coexistence of calcite I and calcite II between 1.46 and 1.78 GPa and of calcite II and calcite III between 2.28 and 3.49 GPa. This observation is in very good agreement with earlier investigations of Van Valkenburg (1965), who observed calcite I and II coexistence in a crystal immersed in a hydrostatic pressure medium. Calcite I single crystals were also observed to persist to pressures of 1.9 GPa in the Raman study of Liu and Mernagh (1990). Because of the coexistence of phases, we believe that measurements made by piston-displacement techniques, as in the studies of Bridgman (1939) and Singh and Kennedy (1974), do not yield accurate values of the transition volumes.

In the coexistence domains, difficulties of data processing were greatly exacerbated, and most data points had to be discarded. In coexistence-free domains, it was possible to fit the volume data of calcite I and calcite III to a second-order Eulerian equation of state (see results Table 5). Assuming $K_0' = 4$, one obtains $K_0 = 69.5 \pm 2.1$ GPa for calcite I and $K_0 = 93.2 \pm 1.9$ GPa, $V_0 = 31.87 \pm 0.17$ cm³/mol for calcite III. Considering the small pressure range in which calcite II is detectable, no isothermal bulk modulus can be reasonably proposed for this phase. The compressibility results obtained for calcite I show a good agreement with the earlier studies of Bridgman (1939) ($K_0 = 73.1$ GPa, $K_0' = 4.15$) and Singh and Kennedy (1974) ($K_0 = 71.1$, $K_0' = 4.17$) and with the acoustic measurements of Dandekar (1968).

On the other hand, the bulk modulus obtained for cal-

TABLE 5. Equation of state parameters of calcite I and calcite III

Reference	K_0 (GPa)	K'_0	V_0 (cm³/mol)	Method
		Calcite I		
Bridgman (1925)	73.1	4.15		piston-cylinder
Dandekar (1968)*	71.6–74.7	5.37		acoustic
Singh and Kennedy (1974)	71.1	4.17		piston-cylinder
Eulerian, second-order	69.5 ± 2.1	4		this work
		Calcite III		
Singh and Kennedy (1974)	51.7	—		piston-cylinder
Martens et al. (1982)	84 ± 0.7	—		gasket method**
Eulerian, second-order	93.2 ± 1.9	4	31.87 ± 0.17	this work

* Adiabatic bulk modulus.
** Volume of the sample estimated from the inside diameter of the diamond-anvil cell gasket and its thickness.

cite III is significantly higher than that of 75.2 GPa at 1.7 GPa, determined from piston-displacement by Singh and Kennedy (1974), and that of 84 ± 0.7 GPa, obtained in a diamond cell from estimations of the volume sample from the inside diameter of the gasket and its thickness (Martens et al., 1982). Bridgman (1939) also measured a low incompressibility for calcite III and had argued that calcite is an atypical compound, in that its high-pressure phase is more compressible than the low-pressure polymorphs. On the contrary, our experiments show a 25% decrease in compressibility at the transition between calcite I and calcite III, a value observed in several B1 → B2 transitions, for instance in KF, KCl, or RbF (e.g., Jeanloz, 1982).

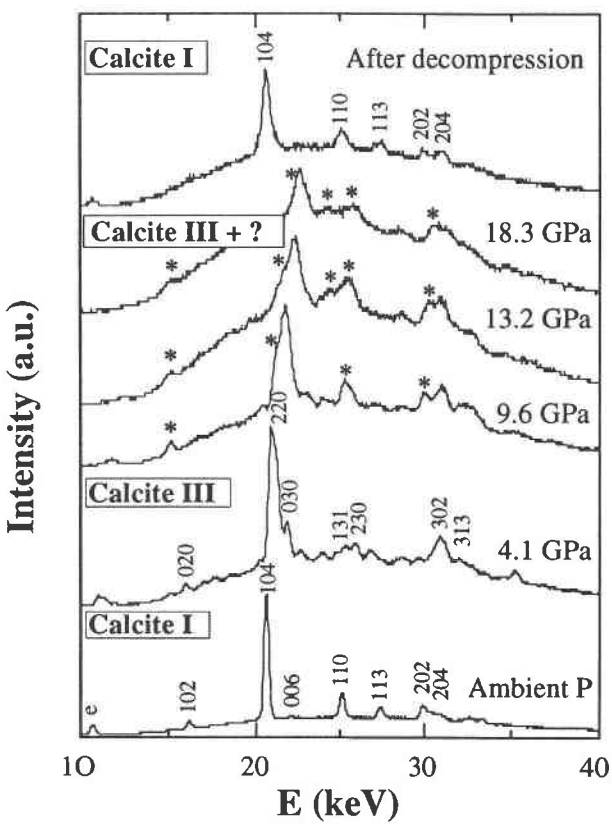

Fig. 10. Evolution of the X-ray powder diffraction spectra of calcite with pressure. Asterisks point out new features appearing above 7 GPa in the patterns.

At pressures exceeding 7 GPa, the patterns of calcite III undergo progressive transformations, as shown in Figure 10. The reflections characteristic of the orthorhombic calcite III, namely 020, 220, 131, 230, and 302, are progressively replaced above 8 GPa by broader peaks (denoted by asterisks in Fig. 10). The presence of aragonite can be excluded by the systematic absence of strong reflections in the range 15–20 keV, where its most intense reflections, 111 and 020, should appear. These changes could be explained by the appearance of a new calcite structure, such as calcite VI indicated in shock wave experiments at about 9.5 GPa (e.g., Tyburczy and Ahrens, 1986). Alternatively, they might represent normal high-pressure features of calcite III, which are not predicted by the simple orthorhombic assignment for this phase. As shown in Figure 10, calcite I was recovered after decompression, and the refined cell parameters were identical to the initial room-pressure values.

ACKNOWLEDGMENTS

D. Andrault is warmly acknowledged for his help during the measurements. The manuscript was greatly improved by the comments of P. Richet and Ph. Gillet, and the critical and constructive reviews of W.A. Bassett and an anonymous reviewer. This work was financially supported by the French program DBT (Minéraux, fluides et cinétiques) and partly by CNRS (URA 726 and URA 734). This is INSU-DBT contribution no. 637.

REFERENCES CITED

Biellmann, C., Gillet, Ph., Guyot, F., and Reynard, B. (1992) Stability and reactivity of carbonates at lower mantle pressures and temperatures. Terra Abstracts, 4, 5.

Biellmann, C., Gillet, Ph., Guyot, F., Peyronneau, J., and Reynard, B. (1993) Experimental evidence for carbonate stability in the Earth's lower mantle. Earth and Planetary Science Letters, 118, 31–41.

Bridgeman, P.W. (1925) The linear compressibility of thirteen natural crystals. American Journal of Science, 15, 287–296.

——— (1939) The high pressure behaviour of miscellaneous minerals. American Journal of Science, 237, 7–18.

Canil, D., and Scarfe, C.M. (1990) Phase relations in peridotite + CO_2 systems to 12 GPa: Implications for the origin of kimberlite and carbonate stability in the Earth's upper mantle. Journal of Geophysical Research, 95, 15805–15816.

Christensen, N.I. (1972) Elastic properties of polycrystalline magnesium,

iron, and manganese carbonates to 10 kilobars. Journal of Geophysical Research, 77, 369–372.

Dandekar, D.P. (1968) Pressure dependence of the elastic constants of calcite. Physical Review, 172, 873.

Davis, B.L. (1964) X-ray diffraction data on two high pressures phases of calcium carbonate. Science, 145, 489–491.

Gillet, Ph. (1993) Stability of magnesite ($MgCO_3$) at mantle pressure and temperature conditions: A Raman spectroscopic study. American Mineralogist, 78, 1328–1331.

Gillet, Ph., Biellmann, C., Reynard, B., and McMillan, P.F. (1993) Raman spectroscopic studies of carbonates. I. High pressure and high temperature behaviour of calcite, magnesite, dolomite and aragonite. Physics and Chemistry of Minerals, 20, 1–18.

Humbert, P., and Plicque, F. (1972) Propriétés élastiques de carbonates rhomboédriques monocristallins: Calcite, magnésite, dolomite. Comptes Rendus de l'Académie des Sciences de Paris, 275, 391–394 (in French).

Irving, A.J., and Wyllie, P.J. (1975) Subsolidus and melting relationships for calcite, magnesite and the join $CaCO_3$-$MgCO_3$ to 36 kb. Geochimica et Cosmochimica Acta, 39, 35–53.

Jeanloz, R. (1982) Effect of coordination change on thermodynamic properties. In S. Akimoto and M.H. Manghnani, Eds., High-pressure research in geophysics, p. 479–498. Center for Academic Publications, Tokyo.

Jeanloz, R., Ahrens, T.J., Mao, H.K., and Bell, P.M. (1979) B1-B2 transition in calcium oxide from shock-wave and diamond-cell experiments. Science, 206, 828–830.

Kalashnikov, N.G., Pavlovski, M.N., Simakov, G.V., and Trunin, R.F. (1973) Dynamic compressibility of calcite-group minerals. Physics of the Solid Earth, 2, 23–29.

Katsura, T., and Ito, E. (1990) Melting and subsolidus phase relations in the $MgSiO_3$-$MgCO_3$ system at high pressures: Implications to evolution of the Earth's atmosphere. Earth and Planetary Science Letters, 99, 110–117.

Katsura, T., Tsuchida, Y., Ito, E., Yagi, T., Utsumi, W., and Akimoto, S. (1991) Stability of magnesite under the lower mantle conditions. Proceedings of Japan Academy, 67B, 57–60.

Kraft, S., Knittle, E., and Williams, Q. (1991) Carbonate stability in the Earth's mantle: A vibrational spectroscopic study of aragonite and dolomite at high pressures and temperatures. Journal of Geophysical Research, 96, 17997–18010.

Lettieri, T.R., Brody, E.M., and Bassett, W.A. (1978) Soft mode dynamics at the pressure-induced ferroelectric transition in sodium nitrate. Solid State Communications, 26, 235–238.

Liu, L.G., and Mernagh, T.P. (1990) Phase transitions and Raman spectra of calcite at high pressures and room temperature. American Mineralogist, 75, 801–806.

Markgraf, S.A., and Reeder, R.J. (1985) High-temperature structure refinements of calcite and magnesite. American Mineralogist, 70, 590–600.

Martens, R., Rosenhauer, M., and Von Gehlen, K. (1982) Compressibilities of carbonates. In W. Schreyer, Ed., High-pressure researches in geoscience, p. 235–238. Schweizerbartsche Verlagsbuchhandlung, Stuttgart, Germany.

Merrill, L., and Bassett, W. (1972) Crystal structures of the high pressure phases of calcite (abs.). Eos, 53, 1121.

——— (1975) The crystal structure of $CaCO_3$ (II), a high-pressure metastable phase of calcium carbonate. Acta Crystallographica, B31, 343–349.

Redfern, S.A.T., Wood, B.J., and Henderson, C.M.B. (1993) Static compressibility of magnesite to 20 GPa: Implications for $MgCO_3$ in the lower mantle. Geophysical Research Letters, 20, 2099–2102.

Reeder, R.J., and Markgraf, S.A. (1986) High-temperature crystal chemistry of dolomite. American Mineralogist, 71, 795–804.

Reeder, R.J., and Wenk, H.R. (1983) Structure refinements of some thermally disordered dolomites. American Mineralogist, 68, 769–776.

Richet, P., Mao, H.K., and Bell, P.M. (1988) Static compression and equation of state of CaO to 1.35 Mbar. Journal of Geophysical Research, 93, 15279–15288.

Ross, C.R. II, and Webb, S.L. (1989) Birch, a program for fitting PV data to on Eulerian finite-strain equation of state. Journal of Applied Crystallography, 23, 439–440.

Ross, N.L., and Reeder, R.J. (1992) High-pressure structural study of dolomite and ankerite. American Mineralogist, 77, 412–421.

Sato, Y., and Jeanloz, R. (1981) Phase-transition in SrO. Journal of Geophysical Research, 86, 11773-11778.

Singh, A.K., and Kennedy, G.C. (1974) Compression of calcite to 40 kbar. Journal of Geophysical Research, 79, 2615–2622.

Tyburczy, J.A., and Ahrens, T.J. (1986) Dynamic compression and volatile release of carbonates. Journal of Geophysical Research, 91, B5, 4730–4744.

Vaidya, S.N., Bailey, S., Pasternack, T., and Kennedy, G.C. (1973) Compressibility of fifteen minerals to 45 kilobars. Journal of Geophysical Research, 78, 6893–6898.

Van Valkenburg, A. (1965) Conférence internationale sur les Hautes Pressions, Le Creusot, France, 2–6 August, (not seen; extracted from Acta Crystallographica, B31, 343, 1975).

Vo Thanh, D., and Lacam, A. (1984) Experimental study of the elasticity of single crystalline calcite under high pressure (the calcite I–calcite II transition at 14.6 kbar). Physics of the Earth and Planetary Interiors, 34, 195–203.

Wells, A.F. (1984) Structural inorganic chemistry (5th edition), 1382 p. Clarendon, Oxford, England.

Williams, Q., Collerson, B., and Knittle, E. (1992) Vibrational spectra of magnesite ($MgCO_3$) and calcite-III at high pressures. American Mineralogist, 77, 1158–1165.

Manuscript received March 30, 1993
Manuscript accepted September 15, 1993